Laser and Particle Beams (2007), *25*, 121–125. Printed in the USA.

DOI: 10.1017/S0263034607070139

Study of laser induced ablation with focused ion beam/scanning electron microscope devices

MARCO BUSSOLI,[1] DIMITRI BATANI,[1] TARA DESAI,[1] FEDERICO CANOVA,[1]
MARZIALE MILANI,[2] MILAN TRTICA,[3] BILJANA GAKOVIC,[3] AND EDOUARD KROUSKY[4]

[1]Dipartimento di Fisica "G. Occhialini," Università di Milano Bicocca, Milano, Italy
[2]Dipartimento di Scienza dei Materiali and "Bombay" FIB/SEM Laboratory, Università di Milano Bicocca, Milano, Italy
[3]Vinca Institute of Nuclear Sciences, Belgrade, Serbia
[4]PALS Research Centre, Prague, Czech Republic

(Received 20 September 2006; Accepted 13 October 2006)

Abstract

We propose the use of Focused Ion Beam/Scanning Electron Microscope (FIB/SEM) devices for the analysis of ablation results. Ablated samples have been obtained by irradiating an Al planar target with an optically smoothed iodine laser working at 0.44 μm. The interpretation of FIB images shows the high potentiality of the technique.

Keywords: Electron emission relaxation region; Ion flux; Laser plasma generation; Laser power; Plasma heating; Plasma interaction; Target heating

INTRODUCTION

Laser ablation is a very active subject of theoretical and experimental investigation, which has been widely studied in the last 20 years, for its intrinsic physical interest, and for its large applications ranging from basic physics investigations to medical and technical applications (Miller, 1994; Beilis, 2007; Bashir, 2007; Alti & Khare, 2006; Schade *et al*., 2006; Thareja & Sharma, 2006; Fernandez *et al*., 2005; Trusso *et al*., 2005; Veiko *et al*., 2006; Wieger *et al*., 2006; Di Bernardo *et al*., 2003; Batani *et al*., 2003; Desai *et al*., 2005; Trtica *et al*., 2006*a*, 2006*b*). Such large interest and its industrial relevance, justifies the development of diagnostics, which are more and more refined, and allows a deeper insight into the ablation process.

Recent advances in laser technologies offer new regimes to the investigation, for instance, the new short-pulse high-intensity regime which is available thanks to the introduction of chirped pulse amplification (CPA) technique, and the introduction of optical smoothing techniques. Particular relevance is also derived from the study of ablation (and damage) process in dielectric transparent materials (for instance, to the construction of very large laser systems like NIF and LMJ). Finally, while lasers can be used for producing ablation, ablation itself can be used as a potential diagnostics in realizing the laser beam characteristics (e.g., measuring laser intensity profile with shots at low-enough laser energy).

In this paper, we propose the use of focused ion beam (FIB) devices for the analysis of ablation in laser irradiated targets, and we present some images (obtained by primary electrons and ions, as explained later) showing the potentiality of this technique, which is largely and routinely used in microelectronics industry (Perrey *et al*., 2004; Phaneuf, 1999; Steer *et al*., 2002; Sivel *et al*., 2004), and now is beginning to find applications in biological imaging (Ballerini *et al*., 1997, 2001; Milani *et al*., 2004, 2005, 2006), but to our knowledge, has never been used for the interpretation/determination of ablated mechanisms based on surface morphology analysis, with partial exceptions (Bleiner & Gasser, 2004; Bleiner & Bogaerts, 2006), unlike the work presented here, using the FIB capabilities only for milling, while the samples were imaged using electron beams.

Our images were recorded using the PALS laser system on an Al target irradiated by an iodine laser (Jungwirth *et al*., 2001; Jungwirth, 2005). The large laser energy available per shot allowed for the use of very large focal spots (while keeping the required laser intensity). Optical smoothing techniques were used because it produced a focal spot which is quite uniform (i.e., free from large size hot spots which could influence the ablation mechanism). This is quite important since experiments are often done by focusing on small focal spots in order to achieve large intensities, thereby, two-dimensional effects affect the results. When optically smoothing is not used, then the beam is characterized as

Address correspondence and reprint requests to: Dimitri Batani, Dipartimento di Fisica "G. Occhialini," Università di Milano Bicocca, Piazza della Scienza 3, Milano 20126, Italy. E-mail: batani@mib.infn.it

"hot spots." The measured ablation parameters are therefore dominated by the effect connected to the short-scale inhomogeneities.

To achieve optical smoothing, we used phase zone plates (PZPs) (Batani *et al*., 2002, 1996; Koenig *et al*., 1994; Stevenson *et al*., 1994), which give the overall shape of the laser intensity distribution in the focal spot, which is flat-top in the central region with Gaussian wings. Therefore, the ablation parameters in the central flat region can be directly compared to analytical results obtained from a one-dimensional model, which by definition assume a spatially uniform intensity. This work is only preliminary/initial, and the only aim is showing the large potentiality of using FIB for the analysis of ablation experimental results.

LASER ABLATION

In our experiment, we irradiated planar Al targets (100 μm thick, 99.99% purity) with an iodine laser using PALS, which delivers a single beam, 29 cm in diameter, with typical energy of 250 J per pulse at 0.44 μm (Jungwirth *et al*., 2001; Jungwirth, 2005). The laser pulse is Gaussian in time with a full width at half maximum (FWHM) of about 350 ps. Of course, such very high energy per pulse was not required, and not used in the present experiment; we limited ourselves to using energies $\leq$ 10 J. However, this energy was still too high and did allow using a very large focal spots for the irradiation of the samples.

The focusing lens had a focal length $f = 600$ mm ($f/2$ aperture). We used PZP in order to produce a uniform irradiation profile without laser hot spots. Since, for technical reasons, it was not possible to produce a PZP with the full size of the laser beam, a smaller PZP was designed to be placed at $f/2$ from the target. The design of our optical system (PZP + focusing lens) implied a focal spot of 400 μm FWHM, with a 250 μm flat region in the center. Samples were irradiated perpendicularly to their surface under vacuum conditions.

THE FIB DEVICE

The FIB apparatus is an extremely important tool in semiconductor manufacturing, which allows for high resolution and sample manipulation during imaging, in particular, sample sectioning along selected planes at selected places, this technique relies on the use of a variable current beam, ranging from pA to nA depending on the type and mode of operation, of metal ions (usually Ga^+ operated at 30 kV) focused and scanned over the surface of the sample. The interaction of the ion beam with the sample results in ejection of atoms from the surface (sputtering), and the production of secondary electrons and ions, which are collected to obtain images. It offers the possibility of changing the plane of observation *in situ* depending on the ongoing collection of information. Imaging resolution lower then 15 nm is possible. The obtained image will show both topographic information and material contrast, and can be used for navigating around the sample. This process can be used to form a cross-sectional view when the sample is tilted and imaged. A further advantage of the FIB/SEM is the presence of an electron column that provide high resolution electron images, that is, when coupled to the ion generated images, can provide detailed information not only on surface, subsurface, and internal morphology, but also on electrical and crystallographic properties.

In the present investigation, we used a FIB/SEM Dual Beam Strata 235 (FEI) and a FIB/SEM Cross beam XL 1540 (Zeiss). All the previously recalled features of the FIB technique (high resolution, navigation, three-dimensional imaging) appear to be viable and useful for the analysis of ablation samples, as it will be shown later.

MEASURING ABLATION WITH FIB

Researchers on laser ablation have contributed to a complex picture of metal removal under energetic laser-pulse action. Depending on pulse intensity, three photo-thermal components can be seen: vaporization, melt displacement, and explosive or volumetric melt ejection. Figures 1 and 2 shows FIB images obtained with two different laser-irradiated Al-samples. Microscopy analysis done by FIB with e- and i-beams, which we will show later, clearly shows melting pool formation, melt displacement, and explosive or volumetric melt ejection of material (Fig. 1). Vaporization or/and laser beam sputtering is dominant (Fig. 2).

The sample in Figure 1 was irradiated with one laser pulse in a vacuum by iodine laser, 440 nm wavelength, intensity $\approx 10^{13}$ W/cm^2, pulse duration (FWHM) = 350 ps. The target was Al (purity 99.99%) and plate thickness 100 μm. PZP were used for intensity profile modification.

The damaged area is composed of four main regions, clearer from the i-beam image of Figure 1B with the central part convex in relation to the surface. Irradiation was accompanied by plasma formation. The ablation in the central zone caused a partial drilling of Al, visible small hole in Figures 1A and 1B.

There is a clear appearance of hydrodynamic structures like re-solidified droplets and splashed melt at the periphery of the central region and the consequence of rapid heating and cooling are visible in all inner crater regions as seen in Figures 1C and 1D. Figure 1E shows the surface structure in a third zone, at larger distances from the central region.

Let's describe in details the ablation based on FIB analysis: The sample in Figure 2 was irradiated with one laser pulse in a vacuum by an iodine laser, 440 nm wavelength, but intensity was below 10^{10} W/cm^2, pulse duration (FWHM) $\tau = 350$ ps. In this case, PZP were not used for intensity profile modifications.

According to Gamaly *et al*. (2002), the ablation threshold in the ps regime for metals is given by $F_{th}\,[\mathrm{J/cm^2}] \approx 0.05\,\tau\,[\mathrm{ps}]^{0.5}$. For $\tau = 350$ ps, we get $F_{th}\,[\mathrm{J/cm^2}] \approx 1$ J/cm^2. Now for Figure 1, the flux on the target is $\approx$ 3500 J/cm^2 (10^{13} W/cm$^2 \times 350$ ps), while for Figure 2, it is 3.5 J/cm^2

https://doi.org/10.1017/S0263034607070139 Published online by Cambridge University Press

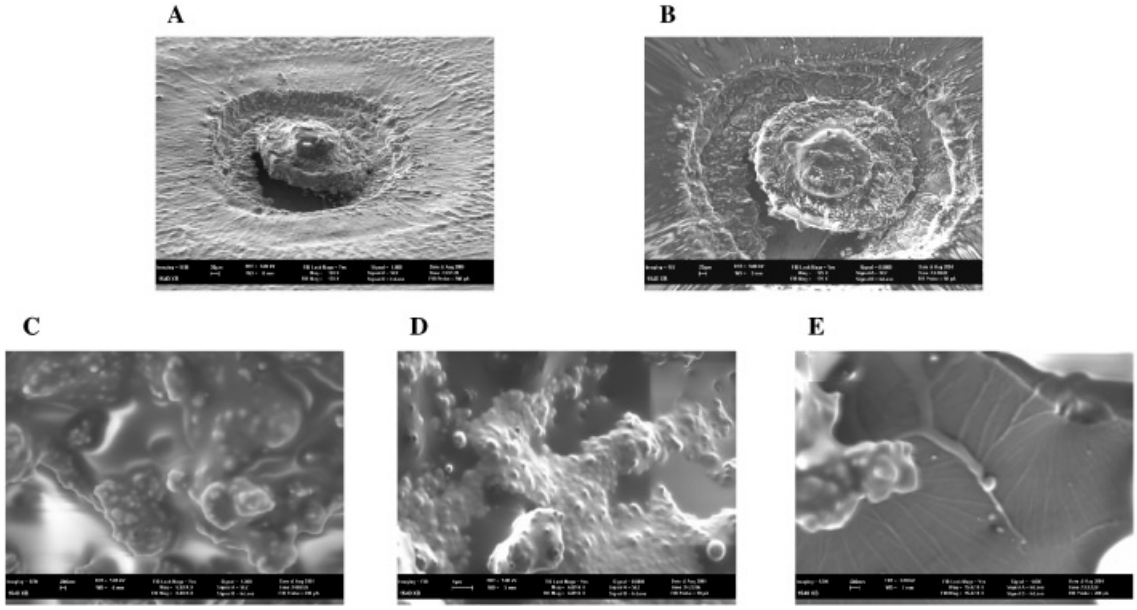

Fig. 1. PALS-Iodine laser-induced morphology changes of aluminum (Al) target. Analysis was carried out by scanning microscopy. Laser parameters: wavelength = 440 nm, pulse duration = 350 ps (FWHM), power density about 10^{13} W/cm^2. (A-E): Aluminum target after one pulse irradiation. (**A**) and (**B**), central part of damaged area recorded with e- and i-beam, respectively. (**C** and **D**), part of second zone, recorded with e- and i-beam, respectively. (**E**), part of third zone, recorded with e-beam.

(10^{10} W/cm^2 × 350 ps). Hence, in the first case we have a flux, which is three orders of magnitude above the ablation threshold, while in the case of Figure 2; it is close to the threshold. Theoretically, it is also possible to calculate the number of ablated atoms per unit surface as $n_{abl} \approx I_L/E_{ib}$, that is, the ratio of laser intensity to the ionic binding energy. For $E_{ib} \approx 4$ eV, we then get $n_{abl} \approx 1.5 \times 10^{31}$ cm^{-2}s^{-1} for the case in Figure 1 ($I_L \approx 10^{13}$ W/cm^2) and $n_{abl} \approx 1.5 \times 10^{28}$ cm^{-2}s^{-1} for the case in Figure 2 ($I_L \approx 10^{10}$ W/cm^2).

Let's consider the second case, by multiplying the laser pulse duration and the measured focal spot size ($\approx$125 μm), we get a total number of ablated atoms $N_{abl} \approx 0.75 \times 10^{16}$, or a number of mole of material removed from the surface $N_{mol} \approx N_{abl}/N_A \approx 1.1 \times 10^{-8}$ (here N_A is the Avogadrro number $\approx 6\ 10^{23}$). Finally, taking into account that for Al, atomic number and density are respectively $A = 27$ and $\rho = 2.7$g/cm^3. We can calculate the volume and by dividing for the surface, we get an ablation depth $\approx$ 550 nm. This qualitatively corresponds to what is shown in Figure 2, that is, an ablation pattern which does not go in depth into the material (in agreement with the fact that we are very close to the ablation threshold).

The same calculation in the case of Figure 1 would give a depth of 550 μm. In reality, the ablation depth is large (as seen in Fig. 1), but not so large. However, we did not expect that the formula $n_{abl} \approx I_L/E_{ib}$, and its implicit linear scaling vs. laser pulse energy, to hold up in such high-pulse-energy relatively-long-pulse case. Indeed various other phenomena will affect the laser plasma interaction (screening by plasma corona, reducing laser absorption; lateral heat transport, increasing the effective ablation surface; etc.).

Coming back to the analysis of the figures, several effects of single pulse action are evidenced in the images:

1. Cleary visible modified region. In the irradiated zone, Figures 2A and 2B, Al surface roughness was changed.
2. After irradiation there is not evidence of melting pool formation.
3. Sharp edge and grainy structure in inner region, probable after sputtering of Al.
4. No evidence of hydrodynamic structures like re-solidified droplets and splashed melt at the periphery.

In summary, we can conclude that vaporization and laser beam sputtering is the main mechanisms in laser ablation, under our conditions. Notice that in Figures 2C and 2D, the FIB apparatus was first used with a high (nA) current of Ga^+ ions allowing sample manipulation, that is, the sectioning of the sample in the vertical direction. This allows for checking the situation and possible changes in the deep layers of the material. In other words, FIB can provide detailed information not only on surface, but also on subsurface and internal morphology, and its electrical and crystallographic properties. Again, this shows the potentiality of the technique.

CONCLUSIONS

In this paper, we have proposed the use of FIB for the analysis of ablation results obtained by irradiating an Al planar target with an optically smoothed iodine laser working at 0.44 μm. Although, the present work is however only preliminary, the interpretation of FIB images shows the high

https://doi.org/10.1017/S0263034607070139 Published online by Cambridge University Press

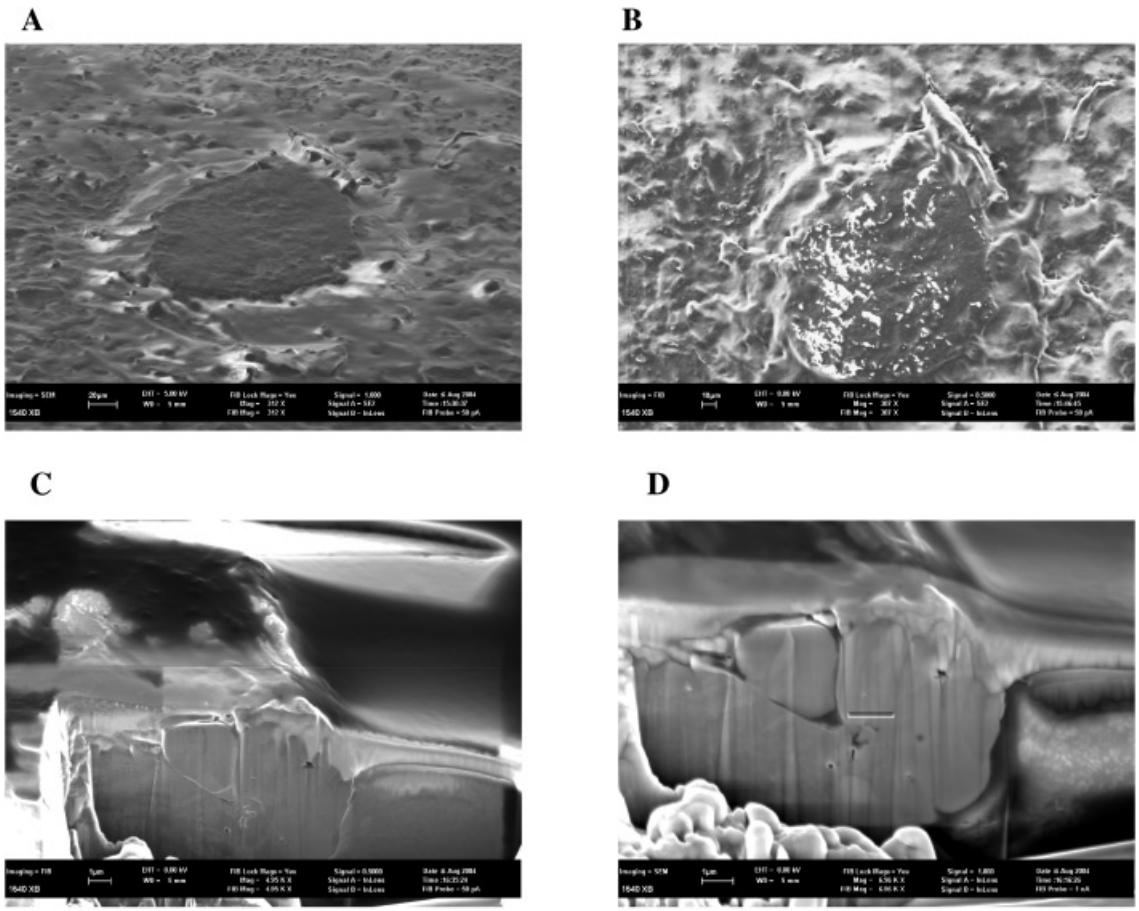

Fig. 2. PALS-Iodine laser-induced morphology changes of aluminum (Al) target. Analysis was carried out by scanning microscopy. Laser parameters: wavelength = 440 nm, pulse duration = 350 ps (FWHM), power density below 10^{10} W/cm^2. (A–E): Aluminum target after one pulse irradiation. (**A**) and (**B**), damaged area recorded with e- and i-beam, respectively. (C and **D**), part of central zone, recorded with e- and i-beam, respectively.

potentiality of using FIB for the analysis of ablation experimental results.

ACKNOWLEDGMENTS

We thank all the PALS team (J. Ullschmied, J. Skala, B. Kralikova, M. Pfeifer, Ch. Kadlec, T. Mocek, A. Präg) and C. Danson and D. Pepler, Rutherford Appleton Laboratory, UK for the PZP.

REFERENCES

Alti, K. & Khare, A. (2006). Low-energy low-divergence pulsed indium atomic beam by laser ablation. *Laser Part. Beams* **24**, 47–53.

Ballerini, M., Milani, M., Batani, D. & Squadrini, F. (2001). Focused ion beam techniques for the analysis of biological samples: A revolution in ultra microscopy? In *Three Dimensional and Multidimensional Microscopy: Image Acquisition and Processing*. Vol. 4261, p. 92. San Jose, CA: SPIE.

Ballerini, M., Milani, M., Costato, M., Squadrini, F. & Turcu, I.C.E. (1997). Life science applications of focused ion beams (FIB). *Eur. J. Histochem.* **41**, 89–90.

Bashir, S. (2007). Laser ablation of ion irradiated CR-39. *Laser Part. Beams* **25**, 181–191.

Batani, D., Bleu, C. & Lower, Th. (2002). Modelistic, simulation, and application of phase plates. *Eur. Phys. J. D* **19**, 231.

Batani, D., Bossi, S., Benuzzi, A., Koenig, M., Faral, B., JBoudenne, J.M., Grandjouan, N., Temporal, M. & Atzeni, S. (1996). Optical smoothing for shock wave generation: Application to the measurement of equation of state. *Laser Part. Beams* **14**, 211–233.

Batani, D., Stabile, H., Ravasio, A., Lucchini, G., Desai, T., Ullschmied, J., Krousky, E., Juha, L., Skala, J., Kralikova, B., Pfeifer, M., Kadlec, C., Mocek, T., Präg, A., Nishimura, H. & Ochi, Y. (2003). Ablation pressure scaling at short laser wavelength. *Phys.Rev. E* **68**, 067403.

Beilis, I. (2007). Laser plasma generation and plasma interaction with ablative target. *Laser Part. Beams* **25**, 53–63.

Bleiner, D. & Bogaerts, A. (2006). Multiplicity and contiguity of ablation mechanisms in laser-assisted analytical micro sampling. *Spectrochimica Acta B* **61**, 421–432.

Bleiner, D. & Gasser, P. (2004). Structural features of laser ablation particulate from Si target, as revealed by focused ion beam technology. *Appl. Phys. A* **79**, 1019–1022.

https://doi.org/10.1017/S0263034607070139 Published online by Cambridge University Press

Desai, T., Batani, D., Rossetti, S. & Lucchini, G. (2005). Laser induced ablation and crater formation at high laser flux. *Rad. Effects Defects Solids* **160**, 595–600.

Di Bernardo, A., Batani, D., Desai, T., Courtois, C., Cros, B. & Matthieussent, G. (2003). High intensity ultra short laser induced ablation of metal targets in the presence of ambient gas. *Laser Part. Beams* **21**, 59–64.

Fernandez, J.C., Hegelich, B.M., Cobble, J.A., Flippo, K.A., Letzring, S.A., Johnson, R.P., Gautier, D.C., Shimada, T., Kyrala, G.A., Wang, Y.Q., Wetteland, C.J. & Schreiber, J. (2005). Laser-ablation treatment of short-pulse laser targets: Toward an experimental program on energetic-ion interactions with dense plasmas. *Laser Part. Beams* **23**, 267–273.

Gamaly, E.G., Rode, A.V., Luther-Davies, B. & Tikhonchuk, T.V. (2002). Ablation of solids by femtosecond lasers: Ablation mechanism and ablation thresholds for metals and dielectrics. *Phys. Plasmas* **9**, 949–957.

Jungwirth, K. (2005). Recent highlights of the PALS research program. *Laser Part. Beams* **23**, 177–182.

Jungwirth, K., Cejnarova, A., Juha, L., Kralikova, B., Krasa, J., Krousky, E., Krupickova, P., Laska, L., Masek, K., Mocek, T., Pfeifer, M., Prag, A., Renner, O., Rohlena, K., Rus, B., Skala, J., Straka, P. & Ullschmied, J. (2001). The Prague Asterix laser system. *Phys. Plasmas* **8**, 2495–2501.

Koenig, M., Faral, B., Boudenne, J.M., Batani, D., Bossi, S. & Benuzzi, A. (1994). Use of optical smoothing techniques for shock wave generation in laser produced plasmas. *Phys. Rev. E* **50**, R3314–R3317.

Milani, M., Batani, D., Ballerini, M., Squadrini, F., Cotelli, F., Lora Lamia Donin, C., Poletti, G., Pozzi, A., Eidmann, K., Stead, A. & Bernardinello, A. (2004). High resolution microscopy techniques for the analysis of biological samples. *Eur. Phys. J.: Appl. Physics* **26**, 123.

Milani, M., Drobne, D., Tatti, F., Batani, D., Poletti, G., Orsini, F., Zullini, A. & Zrimec, A. (2005). Read-out of soft X-ray contact microscopy microradiographs by focused ion beam/scanning electron microscope. *Scanning* **27**, 49–253.

Milani, M., Magni, S. & Tatti, F. (2006). FIB/SEM for soft matter and life sciences. *G.I.T. Imaging Microsc.* **8**, 38–40.

Miller, J.C. (1994). *Laser Ablation—Principles and Applications*. Vol. 28. Berlin: Springer-Verlag.

Perrey, C.R., Carter, C.B., Michael, J.R., Kotula, P.G., Stach, E.A. & Radmilovic, V.R. (2004). Using the FIB to characterize nanoparticle materials. *J. Microsc.* **214**, 222–236.

Phaneuf, M.W. (1999). Applications of focused ion beam microscopy to materials science specimens. *Micron* **30**, 277–288.

Schade, W., Bohling, C., Hohmann, K. & Scheel, D. (2006). Laser-induced plasma spectroscopy for mine detection and verification. *Laser Part. Beams* **24**, 241–247.

Sivel, V.G.M., Van den Brand, J., Wang, W.R., Mohdadi, H., Tichelaar, F.D., Alkemade, P.F.A. & Zandbergen, H.W. (2004). Application of the dual-beam FIB/SEM to metals research. *J. Microsc.* **214**, 237–245.

Steer, T.J., Mobus, G., Kraft, O., Wagner, T. & Inkson, B.J. (2002). 3-D focused ion beam mapping of nanoindentation zones in a Cu-Ti multilayered coating. *Thin Solid Films* **413**, 147–154.

Stevenson, R.M., Norman, M.J., Bett, T.H., Pepler, D.A., Danson, C.N. & Ross, I.N. (1994). Binary-phase zone plate arrays for generation of uniform focal profile. *Opt. Lett.* **19**, 363.

Thareja, R.K. & Sharma, A.K. (2006). Reactive pulsed laser ablation: Plasma studies. *Laser Part. Beams* **24**, 311–320.

Trtica, M., Gakovic, B., Batani, B., Desai, T., Panjan, P. & Radak, B. (2006*a*). Surface modifications of a titanium implant by a picosecond Nd:YAG laser operating at 1064 and 532 nm. *Appl. Surface Sci*. APSUSC-D-06-00399R1.

Trtica, M., Gakovic, B., Maravic, D., Batani, D., Desai, T. & Redaelli, R. (2006*b*). Surface modification of titanium by high intensity ultra-short Nd:YAG laser. *Mater. Sci. Forum* **518**, 167–172.

Trusso, S., Barletta, E., Barreca, F., Fazio, E. & Neri, F. (2005). Time resolved imaging studies of the plasma produced by laser ablation of silicon in O_2/Ar atmosphere. *Laser Part. Beams* **23**, 149–153.

Veiko, V.P., Shakhno, E.A., Smirnov, V.N., Miaskovski, A.M. & Nikishin, G.D. (2006). Laser-induced film deposition by LIFT: Physical mechanisms and applications. *Laser Part. Beams* **24**, 203–209.

Wieger, V., Strassl, M. & Wintner, E. (2006). Pico- and microsecond laser ablation of dental restorative materials. *Laser Part. Beams* **24**, 41–45.